TLR8 in the trigeminal ganglion contributes to the maintenance of trigeminal neuropathic pain

Lin-Xia Zhao
Institute of Pain Medicine, Institute of Nautical Medicine, Nantong University
Xue-Qiang Bai
Department of Human Anatomy, School of Medicine, Nantong University
De-Li Cao
Institute of Pain Medicine, Institute of Nautical Medicine, Nantong University
Xiao-Bo Wu
Institute of Pain Medicine, Institute of Nautical Medicine, Nantong University
Ming Jiang
Institute of Pain Medicine, Institute of Nautical Medicine, Nantong University
Jing Zhang
Institute of Pain Medicine, Institute of Natutical Medicine, Nantong University
Jian-Shuang Guo
Institute of Pain Medicine, Institute of Nautical Medicine, Nantong University
Tong-Tong Chen
Department of Human Aantomy, School of Medicine, Nantong University
Hao Wu
Department of Otolaryngology Head Neck Surgery, The Affiliated Hosptial of Nantong University
Yong-Jing Gao
Institute of Pain Medicine, Institute of Nautical Medicine, Nantong University
Zhi-Jun Zhang (zhzhj@ntu.edu.cn)
Nantong University https://orcid.org/0000-0001-6996-8683

Research

Keywords: TLR8, ERK, p38, proinflammatory cytokines, Trigeminal ganglion, Trigeminal neuropathic pain

Posted Date: February 25th, 2020

DOI: https://doi.org/10.21203/rs.2.24451/v1

Abstract

Background: Trigeminal neuropathic pain (TNP) is a significant health problem whereas the involved mechanism has not been completely elucidated. Toll-like receptors (TLRs) are recently demonstrated to be expressed in the dorsal root ganglion and involved in chronic pain. How TLR8 is expressed in the trigeminal ganglion (TG) after infraorbital nerve injury and whether TLR8 is involved in TNP have not been investigated.

Methods: TNP model was established by the partial infraorbital nerve ligation (pIONL) in mice. The effect of TLR8 and its agonist VTX-2337 on pain hypersensitivity was checked by facial pain behavioral test. The immunostaining, real-time RT-PCR, and western blot were used to evaluate the expression of TLR8, pERK, pp38, and proinflammatory cytokines in the TG. The intracellular concentration of Ca 2+ was detected by the calcium imaging.

Results: TLR8 was persistently increased in TG neurons in pIONL-induced TNP model. In addition, deletion of Tlr8 or knockdown of Tlr8 in the TG attenuated pIONL-induced mechanical allodynia, reduced the activation of ERK and p38, and decreased the expression of proinflammatory cytokines in the TG. Furthermore, intra-TG injection of TLR8 agonist VTX-2337 induced facial pain hypersensitivity. VTX-2337 also increased intracellular calcium concentration, induced activation of ERK and p38, and increased the proinflammatory cytokines expression in the TG.

Conclusions: TLR8 contributes to the maintenance of TNP through increasing MAPK-mediated neuroinflammation. Targeting TLR8 signaling may be effective for the treatment of TNP.

Background

The sensation of nociceptive stimuli is mediated by primary sensory neurons in the dorsal root ganglion (DRG) and trigeminal ganglion (TG), which transmit noxious information to brain via spinal cord and medulla oblongata, respectively. The painful sensation of orofacial area is relayed in the TG, which gives three major branches: the ophthalmic nerve (V1), the maxillary nerve (V2), and the mandibular nerve (V3). Trigeminal neuropathic pain (TNP) is usually a result of injury or disease of one or more nerve branches (usually V2 and/or V3) of the TG and can be triggered by subtle sensory stimuli to the affected side of the face, such as light mechanical touch, brushing teeth, and chewing [1]. TNP is a chronic state and difficult to treat in clinical practice. Understanding the pathophysiology of TNP is essential for the management of the pain.

In recent years, increasing evidence revealed that neuroinflammation is involved in the pathological process of neuropathic pain including TNP [2, 3]. After peripheral nerve injury, neuroinflammation occurs at different anatomical locations on the pain transmission pathway, including TG/DRG and medulla oblongata/spinal cord, which facilitates peripheral sensitization and central sensitization [4–6]. Among the inflammatory mediators, the cytokines such as TNF-α, IL-1β, and IL-6 are well demonstrated to be increased in the peripheral nervous system after nerve injury and enhance neuronal excitability [5, 7–9].

Inhibiting these cytokines using neutralizing antibodies or RNA interference inhibits the neuropathic pain behavior in several neuropathic pain models [5].

Toll-like receptors (TLRs) play a vital role in the innate and adaptive immunoreactivity [10]. After binding with ligands, the TLRs initiate and regulate the inflammatory response via the release of cytokines [11, 12]. The family of TLRs has 12 functional TLRs in mice (TLR1–TLR9 and TLR11–TLR13). Unlike other TLRs, the TLR3, 7, 8, 9 are localized in intracellular compartments the immune system [11, 13]. However, evidence shows that TLR7 is localized on the membrane of DRG neurons and regulates itch transmission [14]. Recently, TLR9 was found to be expressed in the DRG macrophages and contributed to neuropathic pain induced by paclitaxel in male mice [15]. Tlr8 and Tlr7 genes show high homology to each other and are both located on the X chromosome. However, TLR8 is located in the intracellular endoplasmic reticulum (ER), endosomes, and lysosomes of DRG neurons, and plays an important role in the pathogenesis of spinal nerve injury-induced neuropathic pain [16]. How TLR8 is expressed in the TG after infraorbital nerve injury and whether TLR8 is involved in TNP have not been investigated.

The mitogen-activated protein kinases (MAPKs), which include extracellular signal-regulated kinase (ERK), p38, and c-Jun N-terminal kinase (JNK), have been reported to contribute to neuroinflammation and chronic pain [17]. In the DRG, the activation of MAPKs pathway, such as ERK and p38, can increase the expression of IL-1β and IL-6 which involved the postoperative and inflammatory pain [18, 19]. Our earlier study showed that TLR8 agonist activated ERK in the DRG neurons and induced pain hypersensitivity [16]. In this study, we used partial ligation of infraorbital nerve (pIONL) model to examine the role of TLR8 in the TG in the pathogenesis of TNP. We found that TLR8 neurons may facilitate TPN via increasing intracellular calcium, activating ERK and p38, and further increasing the expression of proinflammatory cytokines in the TG after infraorbital injury.

Materials And Methods

Animals and Surgery

ICR male mice weighing 26-30 g were provided by the Experimental Animal Center at Nantong University. *Tlr8*$^{-/-}$ mice were developed by CAYN Company (Suzhou, China). *Tlr7*$^{-/-}$ mice were purchased from Jackson Laboratory (stock number 008380). All animals were housed in standard clear plastic cages under controlled ambient temperature (22-24 °C) with a reversed 12:12 hour dark/light cycle, and allowed ad libitum to access to water and food. The experimental and surgical procedures in this study were reviewed and approved by the Animal Care and Use Committee of Nantong University. Animal treatments were performed in accordance with the guidelines of International Association for the Study of Pain.

The pIONL surgery was made as described by Zhang et al. [20, 21]. In brief, mice were anesthetized with compound anesthetics, and then the oral cavity was opened to locate the left tendon of masseter muscle on the top wall of oral cavity in supine position. In front of the tendon, a 1 mm incision was made to expose the infraorbital nerve. The TNP was established by ligating one half of the infraorbital nerve (ION)

with 6-0 silk suture. The mucous membrane of the incision was adhered with the Tissue Adhensive (3M Vetbond, USA). The sham operation was just made an incision on the mucous membrane without damaging the infraorbital nerve.

DNA extraction and genotyping

About 2 mm diameter of the mouse ear was cut from each *Tl8*$^{-/-}$ or *Tlr7*$^{-/-}$ mouse, and then was used to extract DNA with the phenol-chloroform method. The primers of genotyping for *Tl8*$^{-/-}$ mice are as following: forward primer: 5'-GCA GTT GAC GAT GGT TGC ATT-3', and reverse primer: 5'-TGA CGT GCT TTT GTC TGC TG-3'. A 50 μL reaction volume of PCR amplification buffer was used, including 200 ng DNA, 25 μl 2×Taq PCR MasterMix (Tiangen Biotech), and 1.0 μM TLR8 genotyping primers. Reactions initially were denatured at 95 °C for 5 minutes, 35 cycles at 95 °C for 30 s, 60 °C for 30 s, 72 °C for 30 s, and then the final extension at 72 °C for 2 min. The genotyping protocol of *Tlr7*$^{-/-}$ mice was used as described by Jackson Laboratory. Primers included common forward primer olMR8628: 5'-AGG GTA TGC CGC CAA ATC TAA AG-3', wild type reverse primer olMR8629: 5'-ACC TTT GTG TGC TCC TGG AC-3', and mutant reverse primer olMR8630: 5'-TCA TTC TCA GTA TTG TTT TGC C-3'. For PCR amplification, 200 ng DNA was used in a 50 μL reaction volume containing 25 μl 2×Taq PCR MasterMix (Tiangen Biotech), 0.5 μM primers of olMR8628, olMR8629, and olMR8630. Reactions initially were denatured at 94 °C for 2 minutes, 10 cycles at 94 °C for 20 s , 65 °C for 15 s (-0.5 °C per cycle decrease), 68 °C for 10 s, and then 28 cycles at 94 °C for 15 s , 60°C for 15 s, 72 °C for 10 s, and then the final extension at 72 °C for 2 min. Amplicons were separated using 1.5% agarose gel, stained with DuRed (Biotium) and photographed with GelDoc-It Ts Imaging System (UVP, USA).

Drugs and administration

VTX-2337 was purchased from Active Biochem (Hongkong, China). *Tlr8* siRNA and negative control siRNA (NC siRNA) were designed by RiboBio [16]. RVG-9R peptide was purchased from AnaSpec (USA). For peri-infraorbital nerve injection, the *Tlr8* siRNA (2 μg) or NC siRNA was mixed with RVG-9R peptide (molar ratio=1:10) [16, 22]. Intra-TG injection was performed with a 29 G syringe (Becton, Dickinson and Company, USA). After deeply anesthetized with the isoflurane, the head of mouse was hold by one hand. The tip of needle was inserted subsequently through the infraorbital foramen, infraorbital canal and foramen rotundum, finally was positioned in the TG [23]. Different doses (10 ng. 50 ng, and 100 ng) of VTX-2337 (5 ml) were slowly injected.

Facial pain behavioral test

The behavioral test environment was kept at 22-24 °C and 40-60% humidity. Before facial behavioral test, the mice habituate the behavioral test cage for 30 min every day for three days in the behavioral test environment. The von Frey filaments (0.02 g and 0.16 g) were used to stimulate whisker pad innervated by the ION, and the response of the mice was recorded. Each filament was applied three times on the ipsilateral whisker pad. The mean score of three measurements was calculated according to the following criteria: score 0, no response; score 1, exploratory behavior - the mice detect the von Frey

filament; score 2, slight withdrawal response - the mice slowly move their face backward to the stimulation; score 3, quick and intense withdrawal response with lifting paw; score 4, wiping face with forepaw less than three times toward the stimulated facial area; score 5, wiping face with forepaw more than three times toward the stimulated facial area [24, 25].

RNA collection and Real-time RT-PCR

According to the manufacture's protocol of TRIzol reagent (Invitrogen, Carlsbad, CA, USA), the total RNA in TG tissue was collected. The quality and quantity of RNA was checked on the NanoDrop spectrophotometer (Thermo Fisher Scientific, USA). The cDNA was reversed from RNA using the first Strand cDNA Synthesis Kit (Takara, Japan). Real-time PCR was performed in A&B Applied Biosystems using the SYBR Green Master Mix (Vazyme, China). The following primers were used in PCR reaction: TLR8 forward: 5'-ACC TGA GCC ACA ATG GCA TTT AC-3', and TLR8 reverse: 5'-TTG CCA TCA TTT GCA TTC CAC-3'; TNF-a forward: 5'-GTT CTA TGG CCC AGA CCC TCA C-3', TNF-a reverse: 5'-GGC ACC ACT AGT TGG TTG TCT TTG-3'; IL-1β forward: 5'-TCC AGG ATG AGG ACA TGA GCA C -3', IL-1β reverse: 5'-GAA CGT CAC CCA GCA GGT TA-3'; IL-6 forward: 5'-CCA CTT CAC AAG TCG GAG GCT TA-3', and IL-6 reverse: 5'-CCA GTT TGG TAG CAT CCA TCA TTT C-3'; GAPDH forward: 5'-AAA TGG TGA AGG TCG GTG TGA AC-3', and GAPDH reverse: 5'-CAA CAA TCT CCA CTT TGC CAC TG-3'. The condition of PCR amplifications was set at 95 °C for 30 s, and then 40 cycles (5s for 95 °C and 30 s for 60 °C). The PCR data were analyzed with StopOne Software v2.3 to show graph. Melt curves were used to judge the specificity of PCR products. Quantification was performed by normalizing cycle threshold (Ct) values with GAPDH Ct and analyzed with the $2^{-\Delta\Delta Ct}$ method.

Immunofluorescence

After deeply anesthetized with the isoflurane, the mice were transcardially perfused with 0.01 M PBS, followed by 4% paraformaldehyde in 0.01 M PBS. The TG was dissected carefully and postfixed in the fixative solution overnight, and then was placed in 30% sucrose in 0.01 M PBS for 2 d. The TG was embedded in OCT solution and then cut into 15 mm sections in a cryostat (Lecia, Germany). These sections were processed for immunofluorescence as we described previously [16]. In brief, the sections were blocked by 5% donkey serum in PBS at room temperature for 1 h. Subsequently, these sections were incubated with primary antibodies against TLR8 (rabbit, 1:500, BosterBio), CGRP (mouse, 1:1000, Sigma-Aldrich), NF200 (mouse, 1:500, Cell Signaling Technology) in a humidified box at 4 °C overnight. Following three rinses with 0.01 M PBS, these sections were further incubated with the secondary antibodies DAR-CY3 (1:1000, Jackson ImmunoResearch) and DAM-488 (1:1000, Jackson ImmunoResearch) or IB4-FITC (1:200, Sigma-Aldrich). The fluorescence signals were checked and captured with fluorescence microscope (Nikon Eclipse Ni-E, Japan). The fluorescence images were analyzed with Image J software (NIH, USA).

Western blot

The TG tissue in WT and *Tlr8*$^{-/-}$ mice was collected, and homogenized in a lysis buffer containing protease and phosphatase inhibitors (Sigma). The protein concentration was checked using BCA Protein Assay (Pierce Biotechnology, USA). The 30 μg protein was loaded in each lane of SDS-PAGE gel, and then transferred to Polyvinylidene-Fluoride (PVDF) membrane. After blocked by 5% skim milk, the PVDF membrane was incubated with the primary antibody against pERK (rabbit, 1:500, Cell Signaling Technology), ERK (rabbit, 1:500, Cell Signaling Technology), p-p38 (rabbit, 1:500, Cell Signaling Technology), p38 (rabbit, 1:500, Cell Signaling Technology). The PVDF membrane was further incubated with IRDye 800CW secondary antibody (goat-anti-rabbit, 1:10000, LI-COR) and captured the images with Odyssey CLx system (Odyssey, USA). The size of bands was evaluated by the prestained protein marker (Thermo Fisher Scientific), and the intensity of bands was calculated by the Image J software (NIH, USA).

HEK293 Cell Culture and Transfection

HEK293 cells were cultured in high glucose Dulbecco's modified Eagle's medium (DMEM; Bio Whittaker Europe, Vervier, Belgium) with 10% (vol/vol) foetal calf serum (PAA, Linz, Austria) and 0.5% penicillin/streptomycin at 37 °C in a humidity-controlled incubator with 5% (vol/vol) CO_2. Cells were transfected with the TLR8 or control plasmids using Lipofectamine 2000 (Invitrogen, Netherlands) at 80% confluence. Transfected cells were cultured in the same growth medium for 36 h before calcium measurements.

TG Neuron Culture

After anesthesia using isoflurane, the mouse cranium and brain (4-6 weeks old) were quickly removed, and then the TGs were rapidly collected [26]. The meninges and connective tissues on the TG were carefully stripped in an ice-cold oxygenated balanced salt solution (BSS: 125 mM NaCl, 3 mM KCl, 26 mM NaHCO3, 1.25 mM NaH2PO4, 10 mM glucose, 2.4 mM CaCl2, 1.2 mM MgCl2, 5 mM HEPES, pH 7.2 and osmolarity: 300 mOsm), and each TG was shredded with scissors. These TG tissues were kept at 37 °C for 90 min in the oxygenated aCSF which contained collagenase (3.0 mg/ml, Roche) and dispase-II (2.4 units/ml, Roche), and then were washed with standard aCSF twice. TG Neurons were separated mechanically by polished glass pipettes, and cultivated on the adhesive coverslips (diameter, 13mm) in the 24-well plates. The dissociated TG neurons in each well were incubated in the aCSF at 37 °C (humidified 95% O_2 and 5% CO_2). After 24 h incubation in the carbon dioxide cell incubator chamber, TG neurons were used for calcium imaging measurements.

Ca^{2+} Imaging

HEK 293 cells or TG neurons were loaded with Fura-2AM (2 μM, Molecular Probes) mixed with 0.02% pluronic (Life technologies) for 90 min at RT in a dark circumstance. Coverslips with HEK 293 cells or TG neurons were washed with BSS, and then placed on an inverted fluorescence microscope (Olympus IX73, Japan). The fluorescence emission at 510 nm with excitation at 340 nm and 380 nm was detected at 2 s intervals using a computer-controlled F4500 fluorescence spectrophotometer (Hitachi, Japan). Wavelength selection and the timing of excitation and acquisition of images were controlled using the

Metafluor program (Molecular Devices). Digital images were stored on hard disk for off-line analysis. The ratio of fluorescence intensities (λ340/λ380) at these two wavelengths was recorded as a relative level of intracellular Ca^{2+}.

Quantification and statistics

All results were showed as mean ± SEM. The behavioral data were analyzed by two-way repeated measures (RM) ANOVA followed by Bonferroni test as the post-hoc multiple comparison analysis. For the analysis of $TLR8^{+}$ neurons in the TG, the immunofluorescent images of TG were captured, and then the number of TG neurons was counted using a computer-assisted imaging analysis system (Image J). For western blot, the density of specific bands was measured with Image J, and the intensity of the background was subtracted in each lane. The levels of pERK, pp38 were normalized to total ERK and p38, respectively. Differences between groups were compared using one-way ANOVA followed by Bonferroni test or using Student's t-test if only 2 groups were applied. The criterion for statistical significance was set at $P < 0.05$.

Results

TLR8 expression was increased in TG neurons after pIONL-induced TNP

Before and after pIONL, we used the numerical value of face score, which was induced by 0.02 g and 0.16 g von Frey filaments stimulating the whisker pad, to evaluate the degree of TNP [24]. Behavioral data showed that pIONL increased the face score stimulated with 0.02 g (Fig. 1A) and 0.16 g (Fig. 1B) von Frey filaments, starting from Day 3 and lasting more than 28 days after operation ($P < 0.05$ or 0.01 or 0.001, vs. Sham, two-way RM ANOVA followed by Bonferroni test. Fig. 1A, B). We then check the expression of TLR8 in the TG after pIONL. The real-time PCR showed that the expression of *Tlr8* mRNA was increased at Days 3, 10, and 21 after pIONL ($P < 0.05$ or 0.01 or 0.001, vs. Sham, Student's t-test, Fig.1C). Immunofluorescence staining showed that a few $TLR8^{+}$ cells were scattered in the TG of naïve and sham-operated mice, and $TLR8^{+}$ cells were significantly increased at pIONL Day 10 ($P < 0.001$, pIONL vs. sham, Fig. 1D-H). The cell-size distribution showed that TLR8 was expressed mainly in small-diameter neurons (< 300 μm^2, 70.8%), moderately in medium-diameter neurons (300-600 μm^2, 27.8%), and rarely in large-diameter neurons (> 600 μm^2, 1.4%, Fig. 1E). Further double staining showed that TLR8 was colocalized with nonpeptidergic maker IB4, and peptidergic marker CGRP, but rarely with large-diameter neuronal marker NF200 (Fig. 1I-K). These data suggest that TLR8 is expressed in small-diameter neurons in the TG and increased after pIONL.

Deletion or knockdown of *Tlr8* in the TG alleviates pIONL-induced mechanical allodynia

To examine whether TLR8 is involved in TNP, we compared mechanical allodynia after pIONL in WT and $Tlr8^{-/-}$ mice. As shown in Fig. 2A, B, the face score evoked by either 0.02 g or 0.16 g von Frey filament was significantly decreased from 7 d after pIONL till the end of observation period in $Tlr8^{-/-}$ mice ($P < 0.01$ or

0.001, *Tlr8*$^{-/-}$ vs. WT, two-way RM ANOVA followed by Bonferroni test), suggesting the alleviation of the TNP after *Tlr8* deletion. To further check if TLR8 in the TG is involved in TNP, we specifically knocked down TLR8 expression in the TG by intra-infraoribtal nerve injection of *Tlr8* siRNA mixed with RVG-9R [16]. The injection of *Tlr8* siRNA at pIONL 4 d caused a decrease of face score evoked by 0.02 g or 0.16 g von Frey filament. The effect was shown 3 d after the injection and maintained for more than 48 h (P < 0.001, *Tlr8* siRNA vs. NC siRNA, two-way RM ANOVA followed by Bonferroni test, Fig. 2C, D). RT-PCR showed that the injection of *Tlr8* siRNA decreased *Tlr8* mRNA level by 46.2 ± 14.7% 24 h after the injection (P < 0.05, vs. NC siRNA, Student's t-test. n=5 for each group). These data suggest that TLR8 in the TG is involved in the maintenance of TNP.

Deletion of *Tlr8* reduces pIONL-induced activation of ERK and p38 and expression of proinflammatory cytokines in the TG

MAPKs pathway have been well demonstrated in the pathological processes of neuropathic pain [17, 20, 21]. Our previous data showed that ERK and p38, but not JNK were activated in the TG after pIONL [20, 21]. Here we further confirmed the increased expression of pERK and pp38 in the TG 10 d after pIONL in WT mice (P < 0.05 or 0.01, pIONL vs. sham, Student's t-test, Fig. 3A, B). We then compared pERK and pp38 expression in WT and *Tlr8*$^{-/-}$ mice. The results showed that both pERK and pp38 level in the TG of *Tlr8*$^{-/-}$ mice were lower than that in WT mice after pIONL (P < 0.05 WT vs. *Tlr8*$^{-/-}$, Student's t-test, Fig. 3C, D). It suggests that TLR8 is involved in pIONL-induced activation of ERK and p38 in the TG.

The proinflammatory cytokines including TNF-a, IL-1β, and IL-6 have been demonstrated to play an important role in the development and maintenance of neuropathic pain [3, 16, 27]. Our real-time PCR data showed that pIONL increased the expression of TNF-a, IL-1β, and IL-6 in the injured TG of WT mice (P < 0.01 or 0.001, WT-pIONL vs. WT-sham, Student's t-test, Fig. 3E-G). In *Tlr8*$^{-/-}$ mice, the average increasing fold of TNF-a, IL-1β, and IL-6 induced by pIONL is significantly lower than that in WT mice (P < 0.05, *Tlr8*$^{-/-}$-pIONL vs. WT-pIONL, Student's t-test, Fig. 3E-G). These data suggest that pIONL-induced proinflammatory cytokines expression is partially dependent on TLR8 in the TG.

Intra-TG injection of TLR8 agonist VTX-2337 induces pain hypersensitivity

Tlr8 and Tlr7 show high homology with each other, and both recognize viral single-stranded RNA. Several agonists, including CL075, 3M-003, R848 can activate both TLR8 and TLR7 [28-30]. VTX-2337 is a selective and potent agonist for TLR8 [16]. We injected VTX-2337 into the TG to observe the pain hypersensitivity on the face. The behavioral data showed that intra-TG injection of VTX-2337 dose-dependently (50, 100, 500 ng) increased the face score induced by 0.02 g and 0.16 g von Frey filaments (P < 0.05 or 0.01 or 0.001, VTX-2337 vs. PBS, two-way RM ANOVA followed by Bonferroni test, Fig. 4A, B). The pain hypersensitivity emerged 3 h after injection and lasted for more than 6 h. However, the intra-TG injection of VTX-2337 at 100 ng did not induce the pain hypersensitivity in *Tlr8*$^{-/-}$ mice (P > 0.05, two-way RM ANOVA, Fig. 4C, D). However, the pain hypersensitivity was still evoked in *Tlr7*$^{-/-}$ mice (P < 0.01 or 0.001, VTX-2337 vs. PBS, two-way RM ANOVA followed by Bonferroni test, Fig. 4E, F). These data indicate

that TLR8 in the TG is sufficient to induce pain hypersensitivity on face, and also demonstrate that VTX-2337-induced pain hypersensitivity is dependent on TLR8, not TLR7.

TLR8 agonist VTX-2337 increases the calcium concentration in TG neurons

As an important intracellular second messenger, the intracellular Ca^{2+} ($[Ca^{2+}]i$) is involved in many calcium-dependent intracellular signaling pathways. We checked whether VTX-2337 affects the calcium response in HEK293 cell transfected with control or TLR8 plasmid. The calcium image data showed that VTX-2337 had no effect on the HEK293 cells transfected with control plasmid (Fig. 5A). However, VTX-2337 dose-dependently increased the ratio of F340/380 on the HEK293 cells transfected with TLR8 plasmid (Fig. 5B). With the increase of the concentration of VTX-2337, the concentration of $[Ca^{2+}]i$ was also increased (Fig. 5C).

We further examined the effect of VTX-2337 on the $[Ca^{2+}]i$ in primary TG neurons. The data showed that VTX-2337 at 5 mM increased the ratio of F340/380 (Fig. 5D-F). VTX-2337 at 500 nM induced similar $[Ca^{2+}]i$ increase as 5 mM, but 100 nM VTX-2337 induced lower response (Fig. 5G). To test whether TG neurons will desensitize to repeated application of VTX-2337, we applied VTX-2337 three times at 500 s intervals, and the ratio of F340/380 had no difference among the three applications (Fig. 5H). Statistical data showed that the percentage of responded neurons was increased with the concentration increase of VTX-2337 (Fig. 5I), and the fold of the ratio of F340/380 was higher after treatment with 500 nM or 5 mM VXT-2337 than 100 nM VTX-2337 (Fig. 5J).

TLR8 agonist VTX-2337 induces ERK and p38 activation and proinflammatory cytokines expression

To examine whether activating TLR8 can drive activation of ERK and p38 in the TG, we injected VTX-2337 into the TG, and checked the expression of pERK and pp38. Western blot showed that VTX-2337 increased the expression of pERK and pp38 in the TG in WT mice ($P < 0.05$ or 0.001, VTX-2337 vs. PBS, Student's t-test, Fig. 6A, B). However, intra-TG injection of VTX-2337 did not increase pERK and pp38 in the TG of *Tlr8*$^{-/-}$ mice ($P > 0.05$, *Tlr8*$^{-/-}$ vs. WT, Student's t-test, Fig. 6C, D). These data indicate that the activation of ERK and p38 expression induced by VTX-2337 was dependent on TLR8 in the TG.

To check the role of TLR8 in the expression of proinflammatory cytokines, we examined TNF-a, IL-1β, and IL-6 expression in the TG after intra-TG injection of VTX-2337 in WT and *Tlr8*$^{-/-}$ mice. The real-time PCR revealed that VTX-2337 dramatically increased the expression of TNF-a, IL-1β, and IL-6 in the TG in WT mice ($P < 0.01$ or 0.001, vs. PBS, Student's t-test), but not in *Tlr8*$^{-/-}$ mice ($P > 0.05$, vs. PBS, Student's t-test). The increasing fold of TNF-a, IL-1β, and IL-6 in *Tlr8*$^{-/-}$ mice induced by VTX-2337 is lower than that in WT mice ($P < 0.05$ or 0.01, *Tlr8*$^{-/-}$ vs. WT, Student's t-test, Fig. 6E-G), indicating that VTX-2337-induced upregulation of proinflammatory cytokines is dependent on TLR8.

Discussion

In this study, we showed that pIONL induced persistent increase of TLR8 expression in small-size TG neurons, and pIONL-induced pain hypersensitivity was alleviated in *Tlr8*$^{-/-}$ mice or in WT mice treated with *Tlr8* siRNA in the TG. In addition, pIONL-induced neuroinflammation, manifested as MAPKs activation and proinflammatory cytokines production in the TG, was reduced in *Tlr8*$^{-/-}$ mice. Consistently, intra-TG injection of TLR8 agonist VTX-2337 led to facial pain hypersensitivity, the activation of the ERK and p38, and the increase of proinflammatory cytokines expression, which was dependent on TLR8. These results suggest that TLR8 in the TG neurons plays a critical role in the maintenance of TNP.

TLR8 is upregulated in IB4$^+$ and CGRP$^+$ neurons in the TG neurons after pIONL and contributes to the maintenance of TNP

TLRs, as one type of innate receptors, can recognize microbial pathogens and play an essential role in the initiation of innate immune responses [13]. In recent years, the role of TLRs in pain and itch has been widely investigated [14, 31]. Several TLRs have been demonstrated to be expressed in glial cells or neurons in the DRG in chronic pain conditions [15, 32]. For example, TLR9 is expressed in DRG macrophages and contributed to chemotherapy-induced neuropathic pain [15]. TLR3 is expressed in small-diameter TRPV1-positive DRG neurons and regulates sensory neuronal excitability [33]. TLR7 is distributed in TRPA1-positive DRG neurons and involved in both pain and itch [34, 35]. Although it had been reported that TLR8 was nonfunctional in mice [36], increasing evidence has shown that TLR8 in immunocytes and neural cells has effects on the inflammation and neuronal apoptosis [36, 37]. Our previous data showed that TLR8 is expressed in small IB4-positive DRG neurons and contributes to spinal nerve injury-induced neuropathic pain [16, 38].

In contrast to well-studied TLRs in the DRG underlying chronic pain, the expression of TLRs in the TG and the role of TLRs in TNP are less studied. Here we found that TLR8 had low expression in naïve mice but dramatically increased in pIONL-operated mice. In addition, TLR8 was expressed in both IB4$^+$ and CGRP$^+$ small-diameter TG neurons after pIONL. As TLR8 was mainly expressed in IB4$^+$ neurons in the DRG of naïve mice [16], we speculate that pIONL increases TLR8 in IB4$^+$ neurons and induces TLR8 in CGRP$^+$ neurons. Considering that IB4$^+$ and CGRP$^+$ neurons give out C- and Aβ-afferent fibers in peripheral nervous system, and are widely recognized in transmission of noxious signals to spinal cord [16, 39], TLR8 may involve in pain signal processing. Our behavioral data further showed that *Tlr8*$^{-/-}$ mice suffered less mechanical allodynia than WT mice, and knockdown of TLR8 in the TG alleviated the TNP in the late phase (> 7 d), not in the earlier phase (< 3 d), suggesting the involvement of TLR8 in the maintenance of TNP. As TLR8 is expressed in the primary afferents in the spinal cord [16], we do not exclude the possible role of TLR8 in the medulla oblongata in mediating TNP.

TLR8 contributes to the maintenance of TNP via ERK and p38 activation in the TG

In immunocytes, the canonical downstream signaling of TLR8 in endosomal compartments is related with the production of cytokines mediated by NF-κB pathway [14, 32]. However, the signaling pathway of NF-κB in the peripheral sensory neurons cannot be activated by the TLR8 agonist VTX-2337 [16]. Instead,

VTX-2337 induced ERK activation in the DRG after intrathecal injection, and SNL-induced ERK activation was also reduced in *Tlr8*$^{-/-}$ mice, suggesting ERK as a downstream signal of TLR8 in the DRG [16]. It has been shown that ligation of ION induces activation of ERK and p38, but not JNK in the TG [20, 21]. ERK was also activated in the TG neurons induced by migraine or lingual nerve crush [20, 40, 41].We show that pIONL-induced ERK activation was reduced in *Tlr8*$^{-/-}$ mice. Consistently, intra-TG injection of VTX-2337 also induced pain hypersensitivity and pERK action in WT mice, but not in *Tlr8*$^{-/-}$ mice. Similarly, the activation of p38 induced by pIONL was decreased in the *Tlr8*$^{-/-}$ mice, and p38 was also activated by VTX-2337 in TLR8 dependent manner. Given that inhibition of ERK activation by PD98059 (MEK inhibitor) attenuated pIONL-induced mechanical allodynia and lingual nerve crush-induced mechanical allodynia and heat hyperalgesia [20, 41], and intra-TG administration of p38 inhibitor SB203580 alleviated the tongue pain and pIONL-induced TNP [21, 42], TLR8 may contribute to the maintenance of TNP via activation of ERK and p38 in the TG.

TLR8 is involved in neuroinflammation

Neuroinflammation, which is characterized by the production of cytokines and chemokines in the nervous system, is one of hallmarks in neuropathic pain [2-5, 19, 43-45]. Several studies show the increased levels of cytokines TNF-a, IL-1β and IL-6 in the DRG of animals with chronic pain induced by chemotherapeutic paclitaxel, chronic constriction of sciatic nerve, experimental autoimmune encephalomyelitis, operation, and inflammation [18, 46-48]. Decreasing the expression of TNF-a, IL-1β and IL-6 in the DRG can alleviate the neuropathic and inflammatory pain [44, 47, 48]. Intra-TG injection of TNF-α inhibitor Etanercept, or IL-1β inhibitor Diacerein attenuated pIONL-induced mechanical allodynia for up to 6 h [20]. In the present study, pIONL or intra-TG injection of VTX-2337 induced the increase of TNF-a, IL-1β and IL-6 expression in the TG, which was impeded in the *Tlr8*$^{-/-}$ mice, indicating that TLR8 is the upstream of proinflammatory cytokines' production in the TG after pION.

Our previous studies showed that inhibition of ERK with PD98059 decreased pIONL-induced upregulation of TNF-α and IL-1β in the TG [20]. P38-MAPK inhibitor SB203580 also showed similar effect [21]. Therefore, the activation of ERK and p38 in the TG may trigger the production of proinflammatory cytokines to induce TNP. Vice versa, the proinflammatory cytokines can activate the MAPKs pathway to induce pain hypersensitivity in the peripheral sensory neurons. In the DRG, IL-6 can activate ERK signaling to induce pain hypersensitivity [49]. Likely, IL-1β also induced the pain hypersensitivity through activating p38 pathways in the DRG [50, 51]. Regional application of TNF-a at nerve root caused pain hypersensitivity and increased pERK in small and medium size DRG neurons [52]. Therefore, the activation of MAPKs pathway can induce the product of proinflammatory cytokines, which conversely boost the MAPKs pathway in the peripheral sensory ganglions, such as TG and DRG. This whole process creates a vicious circle for neuropathic pain.

TLR8 is involved in the increase of intracellular calcium and may enhance neuronal excitability

Intracellular calcium affects a wide variety of neuronal responses, including neuronal excitability. The neuronal excitability of primary sensory neurons is increased after peripheral nerve injury [2, 19, 39]. Using calcium imaging, we found that TLR8 agonist VTX-2337 rapidly increased $[Ca^{2+}]i$ in HEK293 cells transfected with TLR8 plasmid or primary cultured TG neurons. The increased $[Ca^{2+}]i$ may due to extracellular calcium influx or intracellular calcium release from organelles, such as ER and lysosomes [7, 35, 53-56]. TLR8 is localized in in the ER, endosomes, and lysosomes in human monocytes and macrophages [57, 58]. We recently demonstrated that TLR8 is also distributed in the same organelles in DRG neurons. Thus, we speculate that the increased calcium after VTX-2337 treatment is released from intracellular stores. But how TLR8 mediates calcium release needs further investigation in future.

It has been demonstrated that the increase of intracellular calcium can trigger a myriad of intracellular signals, which include the phosphorylation of MAPK pathways (such as ERK and p38), inflammatory responses, and the release of neurotransmitter [53, 59, 60]. In addition, activated ERK increases the expression of sodium channel Nav1.8, and regulate the TRPV1 activity in the peripheral sensory neurons [61, 62]. Similarly, activated p38 can also directly regulate the phosphorylation of the Nav1.8 channel and increase the level of TRPV1 in the DRG neurons [61, 63]. Furthermore, proinflammatory cytokines upregulate the expression of Nav1.7 and Nav1.6, which contributes to peripheral sensitization and neuropathic pain [64, 65]. Therefore, the activation of TLR8 may increase the neuronal excitability of TG neurons via regulating the expression and function of sodium channel.

Conclusion

In the present study, we demonstrated that pIONL increased TLR8 expression in small-diameter TG neurons. TLR8 may facilitate peripheral sensitization and trigeminal neuropathic pain through increasing intracellular calcium, activating MAPKs, increasing proinflammatory cytokine expression, and enhancing neuronal excitability. Thus, targeting TLR8 and its downstream signals in the TG may raise a novel strategy for the treatment of the TNP.

Abbreviations

TLRs: Toll-like receptors; TNP: Trigeminal neuropathic pain; TG: trigeminal ganglion; DRG: dorsal root ganglion; pIONL: partial infraorbital nerve ligation; ION: infraorbital nerve; MAPKs: mitogen-activated protein kinases; ERK: extracellular signal-regulated kinase; JNK: c-Jun N-terminal kinase; ER: endoplasmic reticulum.

Declarations

Acknowledgements

Not applicable.

Funding

This study was supported by the National Natural Science Foundation of China (NSFC 31970938, 31671091, 31871064, 81571070, and 31700899), and the Natural Science Research Program of Jiangsu Province (BK20171255 and BK20191448), the Qing Lan Project, and Innovation and Entrepreneurship Training Program for College Students in Jiangsu Province (201810304029Z).

Availability of data and materials

The datasets used and or analyzed during the current study are available from the corresponding author on reasonable request.

Authors' contributions

LXZ performed the pIONL model, behavioral testing, and immunofluorescence staining. XQB carried out the pIONL model, real-time PCR, and Western blot. DLC and XBW contributed to cell culture and calcium imaging. MJ and JZ contributed to western blot experiments. JSG and TTC participated in behavioral testing. HW participated in the experimental design. YJG supervised the experiments, and revised the manuscript. ZJZ conceived of the project, analyzed the data, and wrote the manuscript.

Competing interests

The authors declare that they have no competing interests.

Consent for publication

Not applicable.

Ethics approval and consent to participate

All animal procedures performed in this study were reviewed and approved by the Animal Care and Use Committee of Nantong University and were conducted in accordance with the guidelines of the International Association for the Study of Pain.

Author details

1. Institute of Pain Medicine, Institute of Nautical Medicine, Nantong University, Jiangsu 226019, China.
2. Department of Human Anatomy, School of Medicine, Nantong University, Jiangsu 226001, China.
3. Department of Otolaryngology Head Neck Surgery, the Affiliated Hospital of Nantong University, Jiangsu 226001, China.
4. Co-innovation Center of Neuroregeneration, Nantong University, Jiangsu 226001, China.

References

1. Maarbjerg S, Di Stefano G, Bendtsen L, Cruccu G: **Trigeminal neuralgia - diagnosis and treatment.** *Cephalalgia* 2017, **37:**648-657.

2. Ji RR, Chamessian A, Zhang YQ: **Pain regulation by non-neuronal cells and inflammation.** *Science* 2016, **354:**572-577.
3. Zhang ZJ, Jiang BC, Gao YJ: **Chemokines in neuron-glial cell interaction and pathogenesis of neuropathic pain.** *Cell Mol Life Sci* 2017, **74:**3275-3291.
4. Matsuda M, Huh Y, Ji RR: **Roles of inflammation, neurogenic inflammation, and neuroinflammation in pain.** *J Anesth* 2019, **33:**131-139.
5. Miller RJ, Jung H, Bhangoo SK, White FA: **Cytokine and chemokine regulation of sensory neuron function.** *Handb Exp Pharmacol* 2009**:**417-449.
6. Ji RR, Nackley A, Huh Y, Terrando N, Maixner W: **Neuroinflammation and Central Sensitization in Chronic and Widespread Pain.** *Anesthesiology* 2018, **129:**343-366.
7. Liu Q, Chen W, Fan X, Wang J, Fu S, Cui S, Liao F, Cai J, Wang X, Huang Y, et al: **Upregulation of interleukin-6 on Cav3.2 T-type calcium channels in dorsal root ganglion neurons contributes to neuropathic pain in rats with spinal nerve ligation.** *Exp Neurol* 2019, **317:**226-243.
8. Zhu D, Fan T, Huo X, Cui J, Cheung CW, Xia Z: **Progressive Increase of Inflammatory CXCR4 and TNF-Alpha in the Dorsal Root Ganglia and Spinal Cord Maintains Peripheral and Central Sensitization to Diabetic Neuropathic Pain in Rats.** *Mediators Inflamm* 2019, **2019:**4856156.
9. Zhang J, Su YM, Li D, Cui Y, Huang ZZ, Wei JY, Xue Z, Pang RP, Liu XG, Xin WJ: **TNF-alpha-mediated JNK activation in the dorsal root ganglion neurons contributes to Bortezomib-induced peripheral neuropathy.** *Brain Behav Immun* 2014, **38:**185-191.
10. Abdelsadik A, Trad A: **Toll-like receptors on the fork roads between innate and adaptive immunity.** *Hum Immunol* 2011, **72:**1188-1193.
11. Savva A, Roger T: **Targeting toll-like receptors: promising therapeutic strategies for the management of sepsis-associated pathology and infectious diseases.** *Front Immunol* 2013, **4:**387.
12. Chiu IM: **Infection, Pain, and Itch.** *Neurosci Bull* 2018, **34:**109-119.
13. Kawai T, Akira S: **Innate immune recognition of viral infection.** *Nat Immunol* 2006, **7:**131-137.
14. Liu T, Gao YJ, Ji RR: **Emerging role of Toll-like receptors in the control of pain and itch.** *Neurosci Bull* 2012, **28:**131-144.
15. Luo X, Huh Y, Bang S, He Q, Zhang L, Matsuda M, Ji RR: **Macrophage Toll-like Receptor 9 Contributes to Chemotherapy-Induced Neuropathic Pain in Male Mice.** *J Neurosci* 2019, **39:**6848-6864.
16. Zhang ZJ, Guo JS, Li SS, Wu XB, Cao DL, Jiang BC, Jing PB, Bai XQ, Li CH, Wu ZH, et al: **TLR8 and its endogenous ligand miR-21 contribute to neuropathic pain in murine DRG.** *J Exp Med* 2018, **215:**3019-3037.
17. Ji RR, Gereau RWt, Malcangio M, Strichartz GR: **MAP kinase and pain.** *Brain Res Rev* 2009, **60:**135-148.
18. Gu HW, Xing F, Jiang MJ, Wang Y, Bai L, Zhang J, Li TT, Zhang W, Xu JT: **Upregulation of matrix metalloproteinase-9/2 in the wounded tissue, dorsal root ganglia, and spinal cord is involved in the development of postoperative pain.** *Brain Res* 2019, **1718:**64-74.

19. Ji RR, Xu ZZ, Gao YJ: **Emerging targets in neuroinflammation-driven chronic pain.** *Nat Rev Drug Discov* 2014, **13:**533-548.
20. Zhang Q, Cao DL, Zhang ZJ, Jiang BC, Gao YJ: **Chemokine CXCL13 mediates orofacial neuropathic pain via CXCR5/ERK pathway in the trigeminal ganglion of mice.** *J Neuroinflammation* 2016, **13:**183.
21. Zhang Q, Zhu MD, Cao DL, Bai XQ, Gao YJ, Wu XB: **Chemokine CXCL13 activates p38 MAPK in the trigeminal ganglion after infraorbital nerve injury.** *Inflammation* 2017, **40:**762-769.
22. Berta T, Park CK, Xu ZZ, Xie RG, Liu T, Lu N, Liu YC, Ji RR: **Extracellular caspase-6 drives murine inflammatory pain via microglial TNF-alpha secretion.** *J Clin Invest* 2014, **124:**1173-1186.
23. Neubert JK, Mannes AJ, Keller J, Wexel M, Iadarola MJ, Caudle RM: **Peripheral targeting of the trigeminal ganglion via the infraorbital foramen as a therapeutic strategy.** *Brain Res Brain Res Protoc* 2005, **15:**119-126.
24. Zhang Y, Chen Y, Liedtke W, Wang F: **Lack of evidence for ectopic sprouting of genetically labeled Abeta touch afferents in inflammatory and neuropathic trigeminal pain.** *Mol Pain* 2015, **11:**18.
25. Kernisant M, Gear RW, Jasmin L, Vit JP, Ohara PT: **Chronic constriction injury of the infraorbital nerve in the rat using modified syringe needle.** *J Neurosci Methods* 2008, **172:**43-47.
26. Lee JH, Park CK, Chen G, Han Q, Xie RG, Liu T, Ji RR, Lee SY: **A monoclonal antibody that targets a NaV1.7 channel voltage sensor for pain and itch relief.** *Cell* 2014, **157:**1393-1404.
27. Xu Y, Jiang Y, Wang L, Huang J, Wen J, Lv H, Wu X, Wan C, Yu C, Zhang W, et al: **Thymosin Alpha-1 Inhibits Complete Freund's Adjuvant-Induced Pain and Production of Microglia-Mediated Pro-inflammatory Cytokines in Spinal Cord.** *Neurosci Bull* 2019, **35:**637-648.
28. Spranger S, Javorovic M, Burdek M, Wilde S, Mosetter B, Tippmer S, Bigalke I, Geiger C, Schendel DJ, Frankenberger B: **Generation of Th1-polarizing dendritic cells using the TLR7/8 agonist CL075.** *J Immunol* 2010, **185:**738-747.
29. Gorden KK, Qiu X, Battiste JJ, Wightman PP, Vasilakos JP, Alkan SS: **Oligodeoxynucleotides differentially modulate activation of TLR7 and TLR8 by imidazoquinolines.** *J Immunol* 2006, **177:**8164-8170.
30. Talreja J, Samavati L: **K63-Linked Polyubiquitination on TRAF6 Regulates LPS-Mediated MAPK Activation, Cytokine Production, and Bacterial Clearance in Toll-Like Receptor 7/8 Primed Murine Macrophages.** *Front Immunol* 2018, **9:**279.
31. Ji RR: **Neuroimmune interactions in itch: Do chronic itch, chronic pain, and chronic cough share similar mechanisms?** *Pulm Pharmacol Ther* 2015, **35:**81-86.
32. Liu XJ, Liu T, Chen G, Wang B, Yu XL, Yin C, Ji RR: **TLR signaling adaptor protein MyD88 in primary sensory neurons contributes to persistent inflammatory and neuropathic pain and neuroinflammation.** *Sci Rep* 2016, **6:**28188.
33. Liu T, Berta T, Xu ZZ, Park CK, Zhang L, Lu N, Liu Q, Liu Y, Gao YJ, Liu YC, et al: **TLR3 deficiency impairs spinal cord synaptic transmission, central sensitization, and pruritus in mice.** *J Clin Invest* 2012, **122:**2195-2207.

34. Liu T, Xu ZZ, Park CK, Berta T, Ji RR: **Toll-like receptor 7 mediates pruritus.** *Nat Neurosci* 2010, **13:**1460-1462.

35. Park CK, Xu ZZ, Berta T, Han Q, Chen G, Liu XJ, Ji RR: **Extracellular microRNAs activate nociceptor neurons to elicit pain via TLR7 and TRPA1.** *Neuron* 2014, **82:**47-54.

36. Jurk M, Heil F, Vollmer J, Schetter C, Krieg AM, Wagner H, Lipford G, Bauer S: **Human TLR7 or TLR8 independently confer responsiveness to the antiviral compound R-848.** *Nat Immunol* 2002, **3:**499.

37. Tang SC, Yeh SJ, Li YI, Wang YC, Baik SH, Santro T, Widiapradja A, Manzanero S, Sobey CG, Jo DG, et al: **Evidence for a detrimental role of TLR8 in ischemic stroke.** *Exp Neurol* 2013, **250:**341-347.

38. Wang ZH, Liu T: **MicroRNA21 Meets Neuronal TLR8: Non-canonical Functions of MicroRNA in Neuropathic Pain.** *Neurosci Bull* 2019, **35:**949-952.

39. Berta T, Qadri Y, Tan PH, Ji RR: **Targeting dorsal root ganglia and primary sensory neurons for the treatment of chronic pain.** *Expert Opin Ther Targets* 2017, **21:**695-703.

40. Hawkins JL, Moore NJ, Miley D, Durham PL: **Secondary traumatic stress increases expression of proteins implicated in peripheral and central sensitization of trigeminal neurons.** *Brain Res* 2018, **1687:**162-172.

41. Mikuzuki L, Saito H, Katagiri A, Okada S, Sugawara S, Kubo A, Ohara K, Lee J, Toyofuku A, Iwata K: **Phenotypic change in trigeminal ganglion neurons associated with satellite cell activation via extracellular signal-regulated kinase phosphorylation is involved in lingual neuropathic pain.** *Eur J Neurosci* 2017, **46:**2190-2202.

42. Maruno M, Shinoda M, Honda K, Ito R, Urata K, Watanabe M, Okada S, Lee J, Gionhaku N, Iwata K: **Phosphorylation of p38 in Trigeminal Ganglion Neurons Contributes to Tongue Heat Hypersensitivity in Mice.** *J Oral Facial Pain Headache* 2017, **31:**372-380.

43. Huh Y, Ji RR, Chen G: **Neuroinflammation, Bone Marrow Stem Cells, and Chronic Pain.** *Front Immunol* 2017, **8:**1014.

44. Zhu MD, Zhao LX, Wang XT, Gao YJ, Zhang ZJ: **Ligustilide inhibits microglia-mediated proinflammatory cytokines production and inflammatory pain.** *Brain Res Bull* 2014, **109:**54-60.

45. Wilkerson JL, Gentry KR, Dengler EC, Wallace JA, Kerwin AA, Armijo LM, Kuhn MN, Thakur GA, Makriyannis A, Milligan ED: **Intrathecal cannabilactone CB(2)R agonist, AM1710, controls pathological pain and restores basal cytokine levels.** *Pain* 2012, **153:**1091-1106.

46. Matsuoka Y, Yamashita A, Matsuda M, Kawai K, Sawa T, Amaya F: **NLRP2 inflammasome in dorsal root ganglion as a novel molecular platform that produces inflammatory pain hypersensitivity.** *Pain* 2019, **160:**2149-2160.

47. Zhang X, Jiang N, Li J, Zhang D, Lv X: **Rapamycin alleviates proinflammatory cytokines and nociceptive behavior induced by chemotherapeutic paclitaxel.** *Neurol Res* 2019, **41:**52-59.

48. Zychowska M, Rojewska E, Makuch W, Luvisetto S, Pavone F, Marinelli S, Przewlocka B, Mika J: **Participation of pro- and anti-nociceptive interleukins in botulinum toxin A-induced analgesia in a rat model of neuropathic pain.** *Eur J Pharmacol* 2016, **791:**377-388.

49. Tillu DV, Melemedjian OK, Asiedu MN, Qu N, De Felice M, Dussor G, Price TJ: **Resveratrol engages AMPK to attenuate ERK and mTOR signaling in sensory neurons and inhibits incision-induced acute and chronic pain.** *Mol Pain* 2012, **8:**5.

50. Eijkelkamp N, Heijnen CJ, Carbajal AG, Willemen HL, Wang H, Minett MS, Wood JN, Schedlowski M, Dantzer R, Kelley KW, Kavelaars A: **G protein-coupled receptor kinase 6 acts as a critical regulator of cytokine-induced hyperalgesia by promoting phosphatidylinositol 3-kinase and inhibiting p38 signaling.** *Mol Med* 2012, **18:**556-564.

51. Zelenka M, Schafers M, Sommer C: **Intraneural injection of interleukin-1beta and tumor necrosis factor-alpha into rat sciatic nerve at physiological doses induces signs of neuropathic pain.** *Pain* 2005, **116:**257-263.

52. Takahashi N, Kikuchi S, Shubayev VI, Campana WM, Myers RR: **TNF-alpha and phosphorylation of ERK in DRG and spinal cord: insights into mechanisms of sciatica.** *Spine (Phila Pa 1976)* 2006, **31:**523-529.

53. Bourinet E, Altier C, Hildebrand ME, Trang T, Salter MW, Zamponi GW: **Calcium-permeable ion channels in pain signaling.** *Physiol Rev* 2014, **94:**81-140.

54. Rozas P, Lazcano P, Pina R, Cho A, Terse A, Pertusa M, Madrid R, Gonzalez-Billault C, Kulkarni AB, Utreras E: **Targeted overexpression of tumor necrosis factor-alpha increases cyclin-dependent kinase 5 activity and TRPV1-dependent Ca2+ influx in trigeminal neurons.** *Pain* 2016, **157:**1346-1362.

55. Haustrate A, Prevarskaya N, Lehen'kyi V: **Role of the TRPV Channels in the Endoplasmic Reticulum Calcium Homeostasis.** *Cells* 2020, **9**.

56. Terashima R, Kimura M, Higashikawa A, Kojima Y, Ichinohe T, Tazaki M, Shibukawa Y: **Intracellular Ca(2+) mobilization pathway via bradykinin B1 receptor activation in rat trigeminal ganglion neurons.** *J Physiol Sci* 2019, **69:**199-209.

57. Itoh H, Tatematsu M, Watanabe A, Iwano K, Funami K, Seya T, Matsumoto M: **UNC93B1 physically associates with human TLR8 and regulates TLR8-mediated signaling.** *PLoS One* 2011, **6:**e28500.

58. Ishii N, Funami K, Tatematsu M, Seya T, Matsumoto M: **Endosomal localization of TLR8 confers distinctive proteolytic processing on human myeloid cells.** *J Immunol* 2014, **193:**5118-5128.

59. Canzobre MC, Paganelli AR, Rios H: **Effect of periapical inflammation on calcium binding proteins and ERK in the trigeminal nucleus.** *Acta Odontol Latinoam* 2019, **32:**103-110.

60. Wang H, Wei Y, Pu Y, Jiang D, Jiang X, Zhang Y, Tao J: **Brain-derived neurotrophic factor stimulation of T-type Ca(2+) channels in sensory neurons contributes to increased peripheral pain sensitivity.** *Sci Signal* 2019, **12**.

61. Hudmon A, Choi JS, Tyrrell L, Black JA, Rush AM, Waxman SG, Dib-Hajj SD: **Phosphorylation of sodium channel Na(v)1.8 by p38 mitogen-activated protein kinase increases current density in dorsal root ganglion neurons.** *J Neurosci* 2008, **28:**3190-3201.

62. Zhuang ZY, Xu H, Clapham DE, Ji RR: **Phosphatidylinositol 3-kinase activates ERK in primary sensory neurons and mediates inflammatory heat hyperalgesia through TRPV1 sensitization.** *J Neurosci* 2004, **24:**8300-8309.

63. Ji RR, Samad TA, Jin SX, Schmoll R, Woolf CJ: **p38 MAPK activation by NGF in primary sensory neurons after inflammation increases TRPV1 levels and maintains heat hyperalgesia.** *Neuron* 2002, **36:**57-68.
64. Ding HH, Zhang SB, Lv YY, Ma C, Liu M, Zhang KB, Ruan XC, Wei JY, Xin WJ, Wu SL: **TNF-alpha/STAT3 pathway epigenetically upregulates Nav1.6 expression in DRG and contributes to neuropathic pain induced by L5-VRT.** *J Neuroinflammation* 2019, **16:**29.
65. Tamura R, Nemoto T, Maruta T, Onizuka S, Yanagita T, Wada A, Murakami M, Tsuneyoshi I: **Up-regulation of NaV1.7 sodium channels expression by tumor necrosis factor-alpha in cultured bovine adrenal chromaffin cells and rat dorsal root ganglion neurons.** *Anesth Analg* 2014, **118:**318-324.

Figures

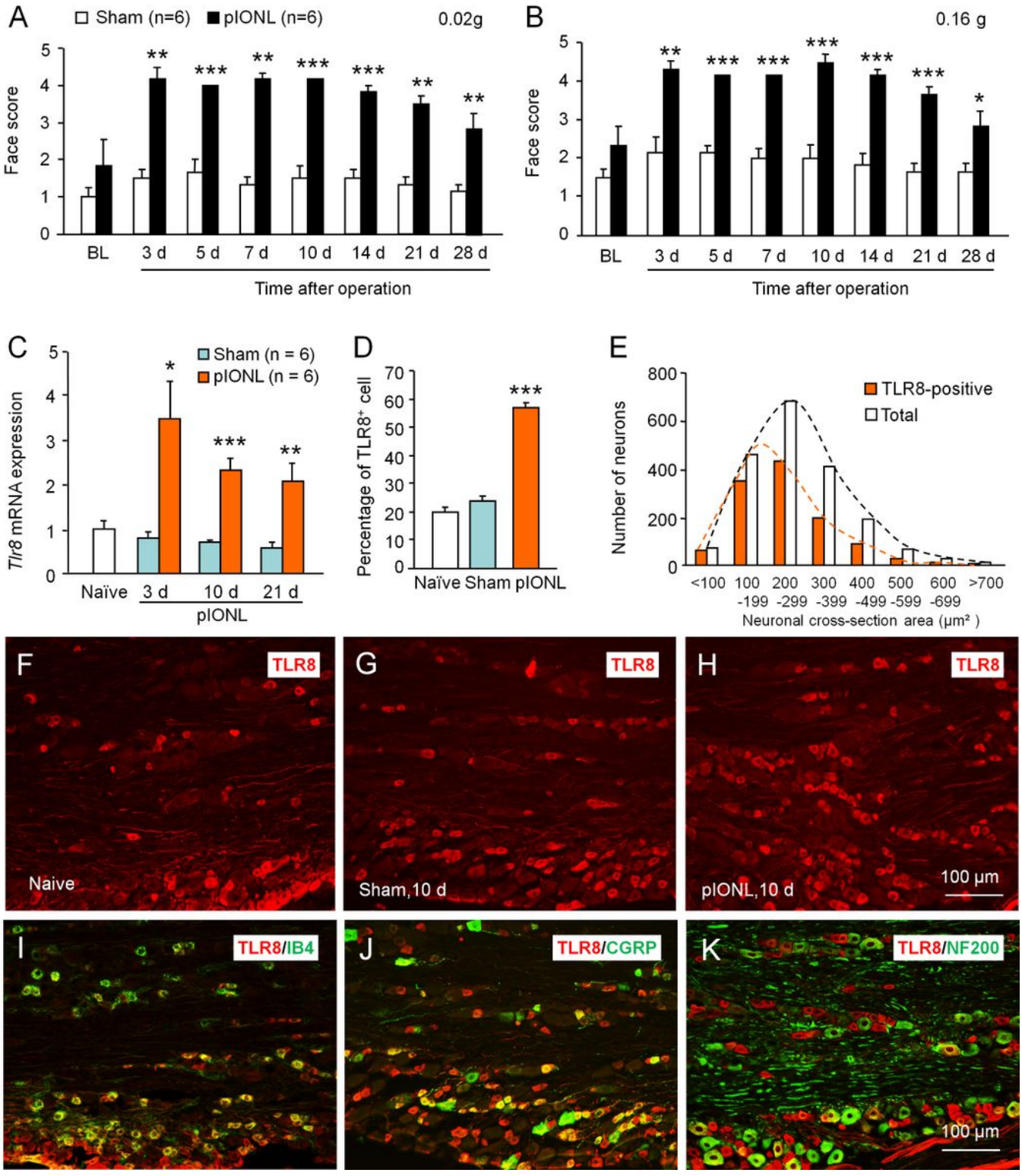

Figure 1

PIONL causes the mechanical allodynia on the ipsilateral facial skin, and increases TLR8 expression in the TG. A, B The time-course of face score stimulated by the 0.02 g von Frey filament (A) and 0.16 g von Frey filament (B) in sham and pIONL mice. * P < 0.05, ** P < 0.01, *** P < 0.001, compared with the corresponding sham group. Two-way RM ANOVA followed by post-hoc Bonferroni test. C The real-time PCR shows the expression of Tlr8 mRNA in naïve, sham and pIONL mice. * P < 0.05, ** P < 0.01, *** P <

0.001, vs. sham. Student's t-test. n = 6 mice/group. D Statistic analysis shows the percentage of TLR8+ neurons in the TG of naïve, sham and pIONL mice. *** P < 0.001, vs. sham. One-way ANOVA followed by Bonferroni test. n =3 mice/group. E Statistic analysis shows the cell-size distribution of TLR8+ neurons and total neurons in the TG at pIONL 10 d. F-H The representative TLR8 immunofluorescent images show the distribution of TLR8+ neurons in the naïve (F), sham (G), and pIONL10 d (H) mice. I-K The double-staining immunofluorescent images show the co-localization of TLR8 with IB4 (I), CGRP (J) and NF200 (K).

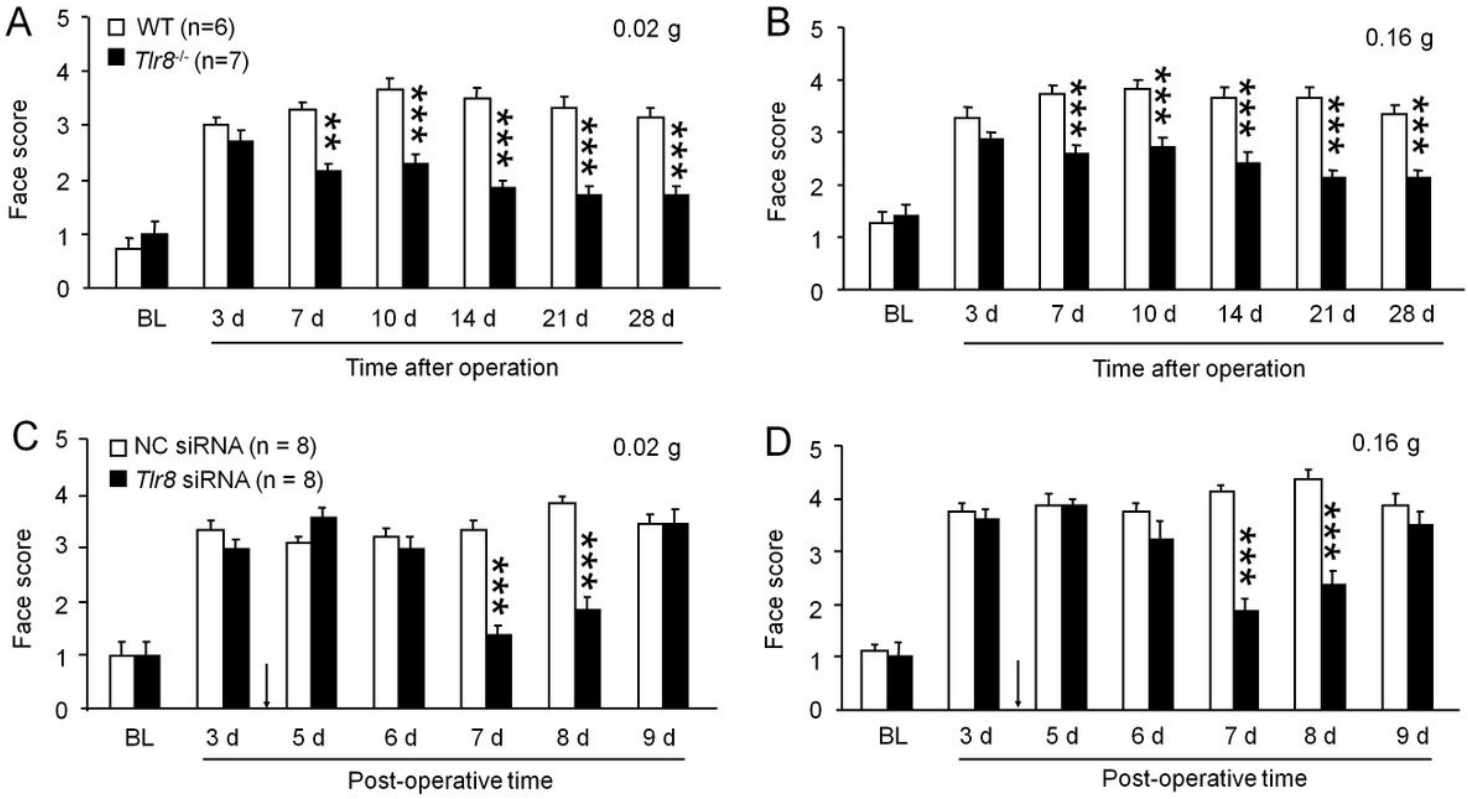

Figure 2

Global deletion of Tlr8 or knockdown of TLR8 in the TG alleviates mechanical allodynia induced by pIONL. A, B The face score stimulated by the 0.02 g von Frey filament (A) and 0.16 g von Frey filament (B) in WT and Tlr8-/- mice. ** P < 0.01, *** P < 0.001, vs. WT. Two-way RM ANOVA followed by Bonferroni test. C, D The face score stimulated by the 0.02 g von Frey filament (C) and 0.16 g von Frey filament (D) after intra-infraorbital nerve injection of Tlr8 siRNA mixed with RVG at pIONL 4 d. *** P < 0.001, vs. NC siRNA. Two-way RM ANOVA followed by Bonferroni test.

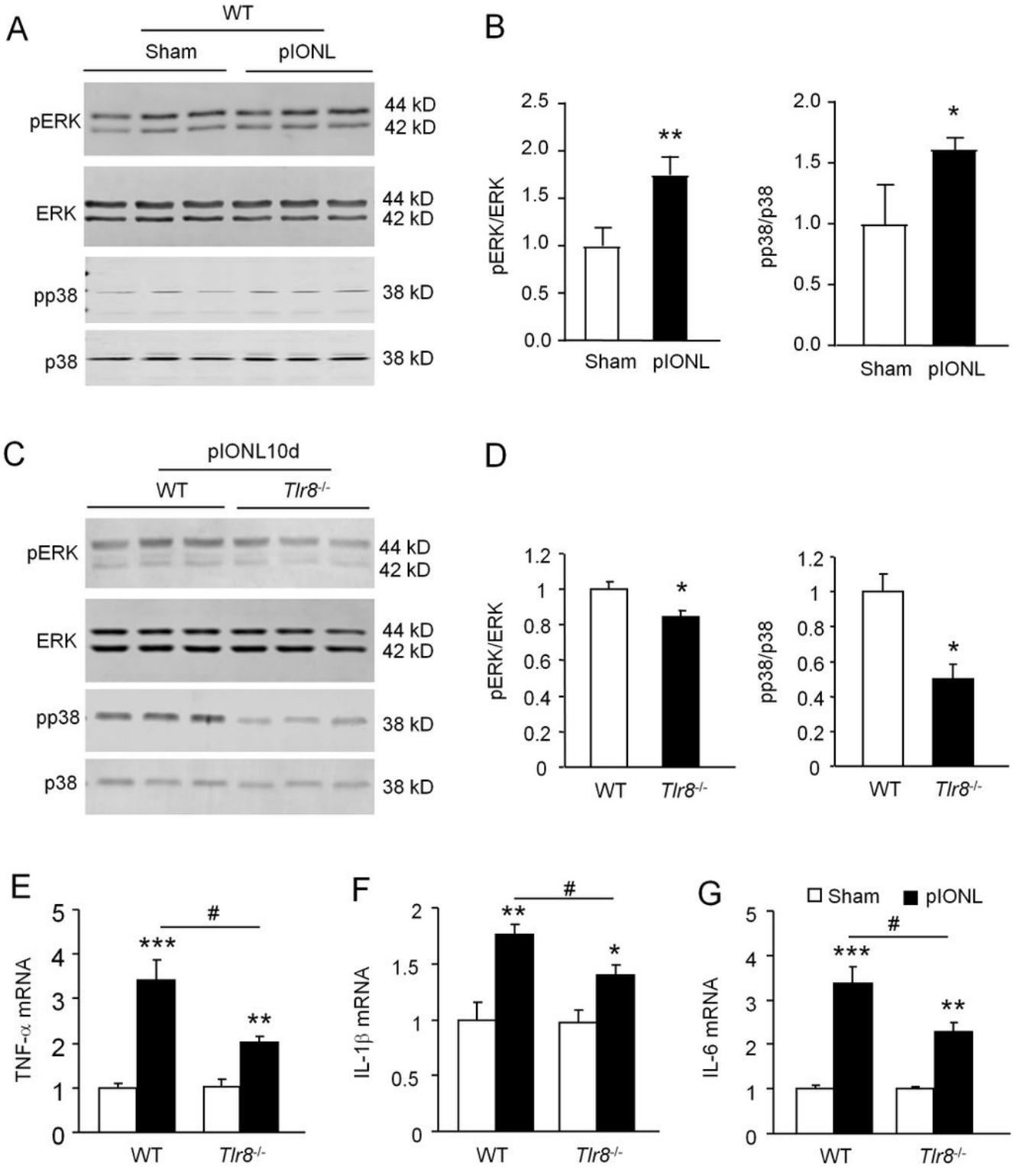

Figure 3

The expression of pERK, pp38, and proinflammatory cytokines induced by pIONL is attenuated in the TG of Tlr8-/- mice. A, B The phosphorylation of ERK and p38 is increased at pIONL 10 d in the TG of WT mice. * P < 0.05, ** P < 0.01, vs. sham. Student's t-test. n=3 mice/group. C, D The phosphorylation of ERK and p38 induced by pIONL is reduced in the TG of Tlr8-/- mice. * P < 0.05, vs. WT. Student's t-test. n=3 mice/group. E-G The expression of TNF-α (E), IL-1β (F), IL-6 (G) is increased by pIONL in the TG of WT

mice. The increasing fold of TNF-α (E), IL-1β (F), IL-6 (G) induced by pIONL is lower in Tlr8-/- mice than that in WT mice. * P < 0.05, ** P < 0.01, *** P < 0.001, pIONL vs. sham. # P < 0.05, Tlr8-/- vs. WT-pIONL. Student's t-test. n=5-6 mice/group.

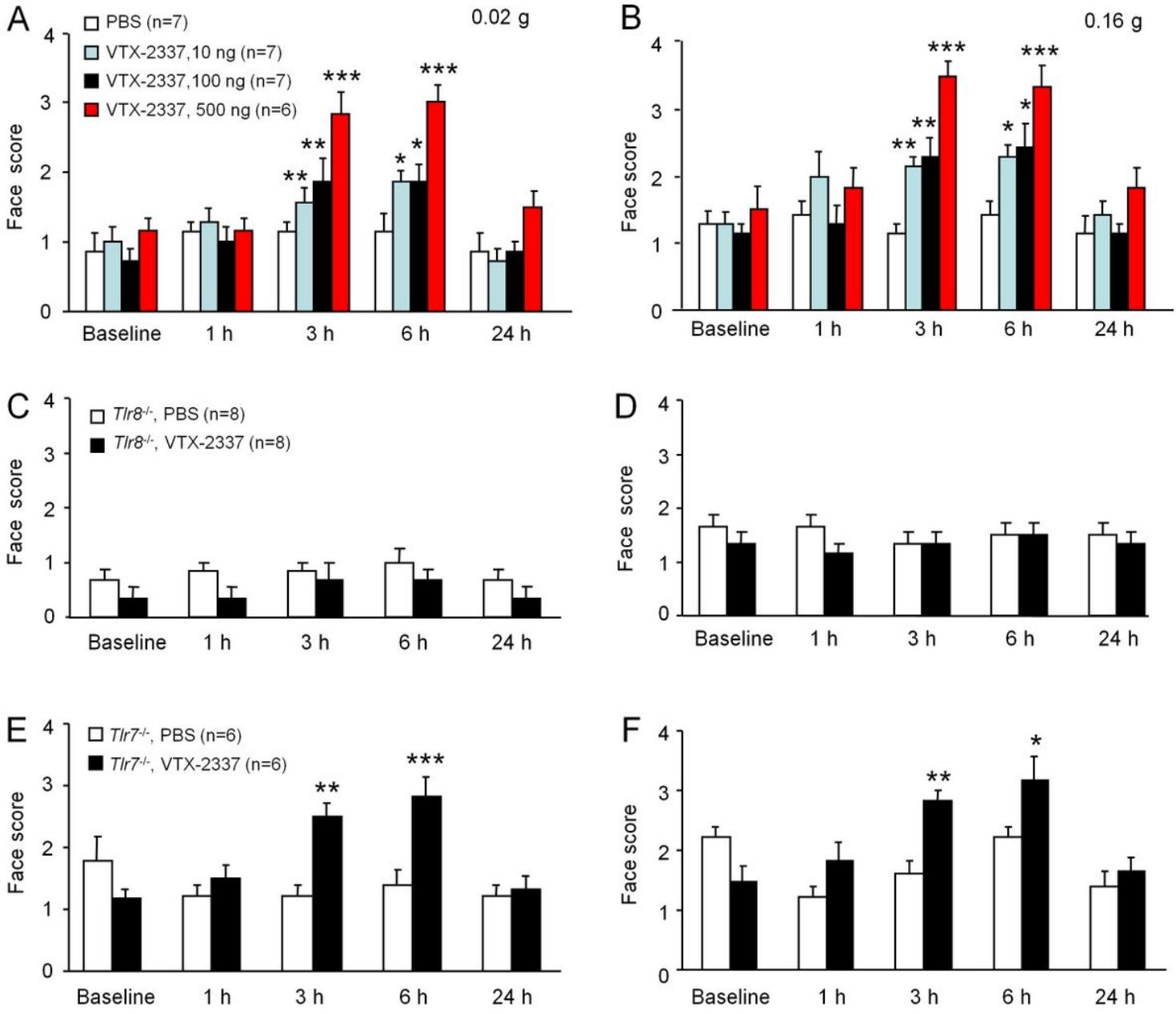

Figure 4

TLR8 agonist VTX-2337 induces pain hypersensitivity in WT and Tlr7-/- mice, but not in Tlr8-/- mice. A, B The face score stimulated by the 0.02 g von Frey filament (A) and 0.16 g von Frey filament (B) after VTX-2337 (10 ng, 100 ng, 500 ng) or PBS injection into TG in WT mice. * P < 0.05, ** P < 0.01, *** P < 0.001, vs. PBS. Two-way RM ANOVA followed by Bonferroni test. C, D The face score stimulated by the 0.02 g von Frey filament (C) and 0.16 g von Frey filament (D) after VTX-2337 (100 ng) and PBS injection in Tlr8-/- mice. E, F The face score stimulated by the 0.02 g von Frey filament (E) and 0.16 g von Frey filament (F)

after VTX-2337 (100 ng) and PBS injection in Tlr7-/- mice. ** P < 0.01, *** P < 0.001, vs. PBS. Two-way RM ANOVA followed by Bonferroni test.

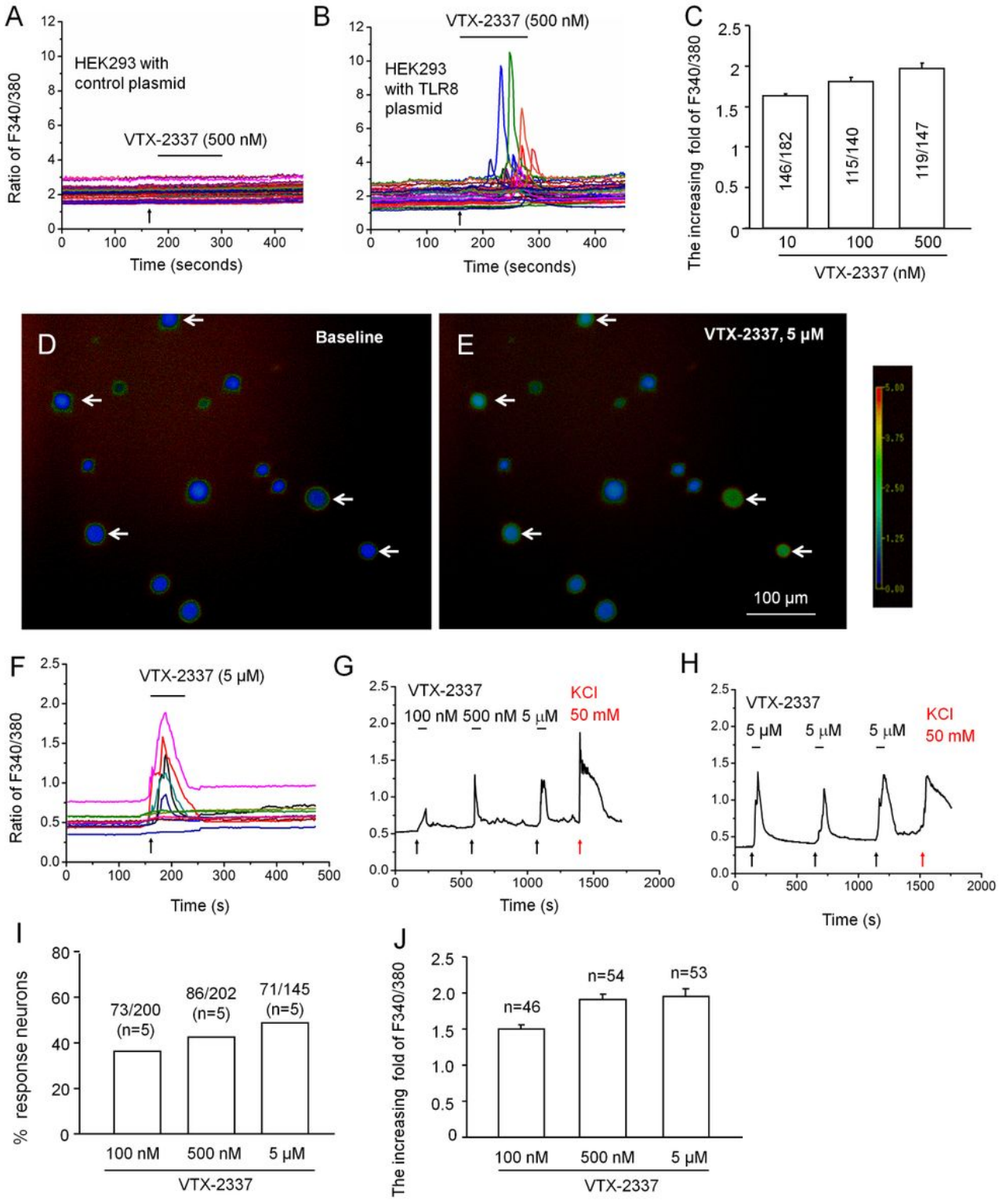

Figure 5

TLR8 agonist VTX-2337 increases the calcium concentration in HEK293 cells transfected with TLR8 plasmid and TG neurons. A, B The effect of VTX-2337 on the ratio of F340/380 in HEK293 cells transfected with control plasmid (A) or TLR8 plasmid (B). C The statistical data show that VTX-2337

dose-dependently increased the ratio fold of F340/380 in HEK293 cells transfected with TLR8 plasmid. D, E The representive calcium images show intracellular calcium activity in TG neurons under baseline condition (D) and the VTX-2337 incubated condition (E). Arrows show the responded neurons to VTX-2337. F The representive curves show the ratio of F340/380 in TG neurons incubated with VTX-2337 (5 M). G The representive curve shows the ratio of F340/380 in one TG neuron incubated with VTX-2337 (100 nM, 500 nM, 5 M) and KCl (50 mM). H The representive curve shows the ratio F340/380 in one TG neuron after incubated with VTX-2337 three times. KCl (50 mM) is used as a positive control. I The statistical data show the percentage of neurons responsive to different concentration of VTX-2337. J The statistical data show the ratio fold of F340/380 after incubation with different concentration of VTX-2337.

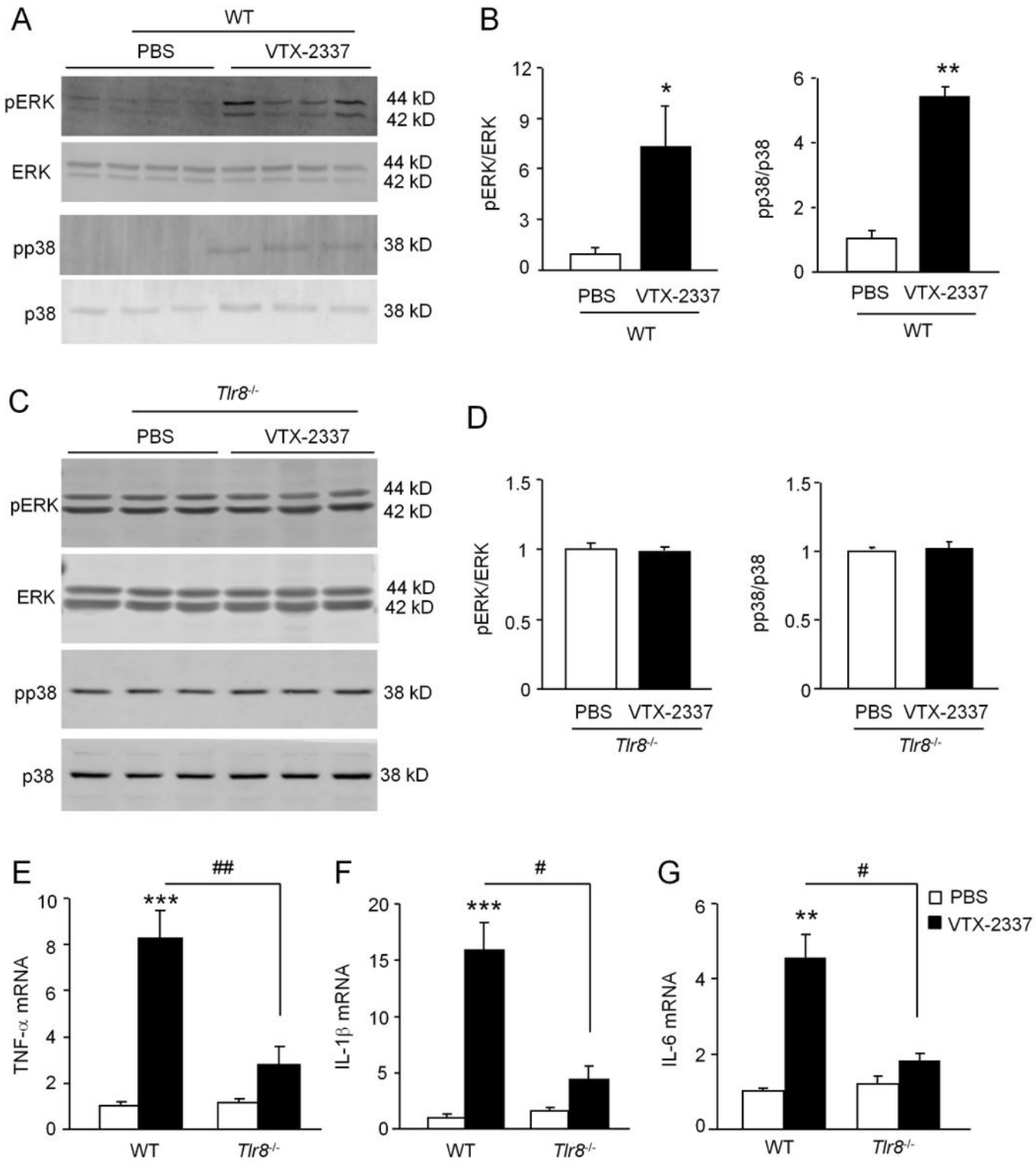

Figure 6

TLR8 agonist VTX-2337-induced upregulation of pERK, pp38, and proinflammatory cytokines is reduced in Tlr8-/- mice. A, B After intra-TG injection of VTX-2337, the phosphorylation of ERK and p38 is increased in the TG of WT mice. * P < 0.05, ** P < 0.01, vs. PBS. Student's t-test. n=3 mice/group. C, D The phosphorylation of ERK and p38 in the TG do not increase after intra-TG injection of VTX-2337 in Tlr8-/- mice. P > 0.05, vs. PBS. Student's t-test. n=3 mice/group. E-G The expression of TNF-α (E), IL-1β (F), IL-6

(G) is increased by intra-TG injection of VTX-2337. The increasing fold of TNF-α (E), IL-1β (F), IL-6 (G) induced by VTX-2337 is lower in Tlr8-/- mice than that in WT mice. ** P < 0.01, *** P < 0.001, vs. WT-PBS. # P < 0.05, ## P < 0.01, vs. WT-VTX-2337 group. Student's t-test. n=5 mice/group.